

Noncontact charge measurement of moving microparticles contacting dielectric surfaces

Alexander Nesterov

German Cancer Research Center, Im Neuenheimer Feld 280, 69120 Heidelberg, Germany and Kirchhoff Institute of Physics, University of Heidelberg, Im Neuenheimer Feld 227, 69120 Heidelberg, Germany

Felix Löffler

Kirchhoff Institute of Physics, University of Heidelberg, Im Neuenheimer Feld 227, 69120 Heidelberg, Germany

Kai König

German Cancer Research Center, Im Neuenheimer Feld 280, 69120 Heidelberg, Germany and Kirchhoff Institute of Physics, University of Heidelberg, Im Neuenheimer Feld 227, 69120 Heidelberg, Germany

Ulrich Trunk

Kirchhoff Institute of Physics, University of Heidelberg, Im Neuenheimer Feld 227, 69120 Heidelberg, Germany

Klaus Leibe, Thomas Felgenhauer, Volker Stadler, Ralf Bischoff, and Frank Breitling

German Cancer Research Center, Im Neuenheimer Feld 280, 69120 Heidelberg, Germany

Volker Lindenstruth and Michael Hausmann

Kirchhoff Institute of Physics, University of Heidelberg, Im Neuenheimer Feld 227, 69120 Heidelberg, Germany

(Received 22 January 2007; accepted 17 June 2007; published online 17 July 2007)

In this study examples for a noncontact procedure that allow the description of instant electric charging of moving microparticles that contact dielectric surfaces, for instance, of a flow hose are presented. The described principle is based on the measurement of induced currents in grounded metal wire probes, as moving particles pass close to the probe. The feasibility of the approach was tested with laser printer toner particles of a given size for different basic particle flow and charging conditions. An analytic description for the induced currents was developed and compared to observed effects in order to interpret the results qualitatively. The implementation of the presented procedure can be applied to transparent and nontransparent particle containers and flow lines of complex geometry which can be composed from the presented basic flow stream configurations.

© 2007 American Institute of Physics. [DOI: [10.1063/1.2756629](https://doi.org/10.1063/1.2756629)]

I. INTRODUCTION

Microparticle transport and manipulation in the gas phase are important features used in many instruments such as airborne particle samplers,¹ electrostatic particle cleaning apparatuses,²⁻⁴ and in new electronic device architectures.^{5,6} In biomedicine and pharmaceutical research, biodegradable microparticles are used as carriers for vaccine delivery, which show a surface charge depending on interaction with cells and cellular components.⁷ Therefore, easy methods that describe particle charging may be helpful for a better control of such techniques.

Nearly all aerosols, albeit natural or artificial, contain electrostatically charged microparticles, and especially some aerosol generation methods generate moderately to highly charged particles.⁸ Electric charging allows spatially defined transport of microparticles within electric fields.

Electrostatic charging occurs by the separation of two contacting solid bodies. Under aerosol conditions, this separation process is affected by particle motion perpendicular or tangential to a contact surface (contact electrification and triboelectric charging, respectively). Although such charging

processes have been studied in many research projects,^{9,10} a generally accepted quantitative description of these phenomena is still missing. One obvious reason for this situation is the complexity of charging effects. The energy states on the contact surface must be determined, but also humidity, electrical breakdown of the surrounding medium (air), and the intensity of the particle contact with the surface must be considered. In many apparatuses, microparticle charging results from both contact electrification and triboelectric charging. Furthermore, the net change in charge of specific materials usually results from the addition of both charging and discharging processes.¹¹⁻¹³ For a deeper understanding of triboelectric charging and the instruments using this effect, it is hence important to have a reliable and easy measuring procedure at hand.

The charge of moving aerosol microparticles is easily determined by induced currents in metal rings.¹⁴⁻²¹ An analytical model for such probing procedures has also been developed.^{15,19} Based on this model, the charge distribution of a discontinuous dust flux has been determined by the height of the current impulses induced by microparticles in a ring-shaped probe. This induced current has been calculated

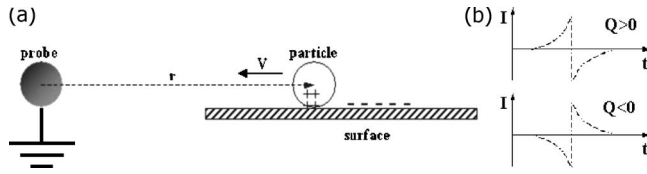


FIG. 1. (a) Schematic representation of measuring principle: A grounded probe is located at the distance r in the electric field of a particle with a charge Q that is moving with a constant velocity v . (b) Qualitative dependency of the induced current I on the time of flight t for positively or negatively charged particles passing the probe. The change in the sign of I marks the time at which the particle position shows the closest approximation to the probe.

and depends on the spatial position of charged particles within the cross section of the ring.^{16,21} As an example, the influence of humidity, temperature, and particle size on the charging of microparticles in pipelined gas flows has been studied by comparison of electrical signals of the inductive ring probes before and after parameter modification.²⁰

The aim of this article is to present a more flexible procedure (consisting of measurement and computer simulation) for the noncontact analysis of microparticle charging that contact along a dielectric surface in a flow stream. The approach uses the effect of induced currents appearing when charged microparticles pass relative to a metal wire probe without contacting the probe. In contrast to other publications, we exploit this well known physical effect to measure the instant charging of microparticles during the contact to surfaces. In the experiments described in the following, a metal wire probe was used which is very compact and thus is applicable in more complicated geometries of particle containers and particle flux lines. The proposed procedure, however, can be also extended to other probe geometries. The proof of principle experiments presented utilized commercially available laser printer toner particles under different aerosol and flow conditions. An analytical model supported by computer simulations reveals a qualitative description of the experimental results.

II. PRINCIPLE OF MEASUREMENT AND SETUP DESIGN

The physical principle describing the measurement is illustrated in Fig. 1(a). Let us consider the electrostatic problem: A charge Q_{ind} is induced in a grounded metal probe by the electric field of a microparticle charged to Q that contacts a dielectric surface. It is assumed that the characteristic sizes of probe and particle are small compared to the distance r between them.

The induced charge Q_{ind} of the probe is in turn proportional to the sum of the electric fields at the location of the probe from the charged dielectric surface E_{sur} and the electric field E_{par} of the microparticle as follows:

$$Q_{\text{ind}} = C_1 [E_{\text{sur}} + (1 - \eta)E_{\text{par}}], \quad (1)$$

where C_1 is a constant depending on the geometrical parameters of the probe and measurement setup, and η is a “phenomenological” constant considering the deviation of the microparticle from a linear trajectory ($\eta=0$) along the surface. This deviation leads to a difference in the contribu-

tion of the particle charge Q and the triboelectrically produced surface charge to Q_{ind} as compared to the expected Q_{ind} value obtained by linear particle movement along the surface.

Further assuming that the electric field of the microparticle is homogenous near the probe results in

$$Q_{\text{ind}} = C_1 \int_{t_0}^t \frac{dQ}{dt'} \frac{1}{4\pi\epsilon r^2(t')} dt' - C_1(1 - \eta) \frac{Q}{4\pi\epsilon r^2(t)}, \quad (2)$$

where the integral in the first summand of Eq. (2) describes the electric field E_{sur} with t_0 being the time at which the particle contacts the surface for the first time and t is the running time value. The second summand in Eq. (2) corresponds to the second summand in Eq. (1) describing E_{par} . Q of the particle has the opposite sign to Q of the surface. If the velocity of the microparticle v is much smaller than c , the vacuum velocity of light ($v \ll c$; which is a realistic assumption for gases and aerosols), and the variables Q and $r = \sqrt{x(t)^2 + y(t)^2 + z(t)^2}$ can be expressed as a function of time t . The induced current I in the probe [Eq. (3)] can be obtained by differentiation of Eq. (2) as follows:

$$\begin{aligned} I = \frac{dQ_{\text{ind}}}{dt} &= \frac{C_1}{4\pi\epsilon} \left[\frac{d}{dt} \int_{t_0}^t \frac{dQ}{dt'} \frac{1}{r^2(t')} dt' - \frac{d}{dt} (1 - \eta) \frac{Q}{r^2(t)} \right] \\ &= \frac{C_1}{4\pi\epsilon} \left[\frac{dQ}{dt} \frac{1}{r^2(t)} - (1 - \eta) \frac{dQ}{dt} \frac{1}{r^2(t)} + (1 - \eta) \frac{2Q}{r^3(t)} \frac{dr}{dt} \right], \\ I = \frac{dQ_{\text{ind}}}{dt} &= \frac{C_1}{4\pi\epsilon} \left[\eta \frac{1}{r^2} \frac{dQ}{dt} + (1 - \eta) \frac{2Q}{r^3} \frac{dr}{dt} \right], \quad (3) \end{aligned}$$

with the linear motion r corresponding to $r = \sqrt{h^2 + v^2 t^2}$, where h is the minimum distance between the probe and the particle, and v the particle velocity.

In the case of triboelectric charging with $\eta=0$, the first summand in Eq. (3) vanishes. The physical meaning of this case is that the contribution to the induced current of the charge increase on the contacted surface is completely compensated by the charge increase on the moving particle. The second summand of Eq. (3) describes the dependence of the induced current I on the particle flow. The arithmetic sign of this element does not only depend on the sign of the charge of the microparticle, but also on the sign of the particle velocity relative to the probe. This means that the induced current is assumed to be positive if a positive particle approaches the probe, and negative if it departs from the probe [Fig. 1(b)]. According to Eq. (3), the induced current decreases with an increasing distance between probe and particle.

The induced charge Q_{ind} can be evaluated from the integral of the induced current along time, $Q_{\text{ind}} = \int I(t) dt$. For $Q_{\text{ind}}=0$, changes of the particle charge due to further triboelectric charging can be neglected.

If multiple particles move close to the probe, the resulting current $I(t)$ can be evaluated as the sum of currents I_n independently induced by the individual particles ($n=1 \dots N$) of the flow as follows:

$$I(t) = \sum_{n=1}^N I_n(Q_n, t + \Delta t_n), \quad (4)$$

whereas N is the amount of particles, and Δt_n the respective delay of each particle. If the particles aggregate or the particle cloud can be regarded as compact, the whole particle cloud can be approximated as a single particle.

In the following, we will show that a simplified computer calculation on the basis of (3) and (4) for $N=2$ or, $N=3$ with appropriately chosen values for the charges Q_1 and Q_2 (and Q_3) allows for reasonable description of the characteristic features of measured current curves $I(t)$. This means that the complex behavior of particle movement and charging can be described by a simplified procedure which is reduced to some major components of the flow stream only. For this description a computer simulation program with a few variables only (mainly N , Q , η , t , v , and h) was written and implemented into MATLAB® (The MathWorks GmbH, Ismaning). Adjusting the parameters to the measured curves, the simulation will help us to understand the charging dynamic of the moving particles.

In the experiments shown here, a metal wire probe was connected to the grounding through an oscilloscope (voltmeter 54622D, Agilent). With this circuit, the induced current $I(t)$ was determined as the quotient of voltage $U(t)$ over internal resistance R_{in} of the oscilloscope $I(t) = U(t)/R_{in}$. It may be pointed out that the precision with which the measurements can be done is highly depending on the sensitivity of the used instrumentation. Nevertheless the principles remain the same.

The measurements were performed with commercially available laser printer toner particles of different colors (OKI Systems GmbH, Düsseldorf, Germany).²² The average diameter of these toner particles was at about 10 μm , as determined by laser diffraction in a Malvern Mastersizer (Malvern Instruments). All particles showed the tendency to agglomerate, by forming bigger and compactly charged compounds. Measurements with the Q/m -meter 210HS-2 (TREC Inc., draw-off method) revealed a negative charge resulting in $Q/m < 10^{-4}$ C/kg for nonactivated laser printer toner particles, i.e., for toner particles that were not subjected to an additional triboelectric charging.

III. RESULTS

In the following, proof of principle experiments based on typical straight and bent flow stream conditions are described and evaluated. Complex flow configurations can be assumed to be composed of these basic elements.

A. Microparticles in a straight and a bent hose

About 30 mg laser printer toner particles were put into a straightened flexible polyamide hose of a diameter $d=6$ mm (Fig. 2, top scheme) using a spatula. A stream of dried air transported the microparticles along the hose. The particle velocity v was adjusted by the air flow in the range between 30 and 75 m/s. Under these conditions, the Reynolds' numbers of the tube ($\text{Re} = vd/\nu$, where

$\nu = 1.5 \times 10^{-5}$ m²/s is the kinematic viscosity of air) were in the range from 12 000 to 30 000, so that turbulent flow conditions dominate particle motion.

The induced current was continuously measured while the microparticles passed the wire probe. In Fig. 2(a) and 2(b), typical current curves are shown in dependency of time. The curves on the left show the experimental measurements, while the curves on the right display the corresponding simulated results. Based on the model assumption of a two particle flow, i.e., the simulations of Eqs. (3) and (4) with $N=2$, the best fit of the experimental peak pattern was obtained. This assumption appears to be reasonable if the induced current of a compact microparticle cloud can be approximated by the induced current of one particle. Comparing the shapes of the experimental and simulated curves it can be concluded that the experimental laser printer toner particle cloud consists of two compact compounds of different sizes.

Simulating the induced current of a single microparticle or compact particle agglomerate, symmetric curves were observed [Fig. 1(b)]. If the particles were negatively charged, the first peak was negative and the second one positive. This agreed well with the experimental data obtained from negatively charged laser printer toner particles. If the particles were positively charged, the first peak was positive and the second negative (data not shown). In most cases additional smaller peaks, certain asymmetries, or smaller first peaks were observed. All these effects were explained by the formation of individual particle agglomerates of different sizes, while the particles were moving in the tube with a relative delay $\Delta t = \Delta t_1 - \Delta t_2$ to each other.

Compared to these results obtained for a straight polyamide hose no qualitative differences were observed in the induced currents when the particles were moving in a boron silicate glass tube (JENAer GLASTTM) of 5 mm diameter.

The experimental setup of a bent hose is schematically shown in Fig. 3 (top image). In this setup, two wire probes (1 and 2) were used. The first probe was located in the bent part of the hose, and the second one in the rear straight part of the hose. In Fig. 3 the two left curves correspond to the experimentally measured induced currents at probes 1 and 2. The absolute current values of the peak maxima at probe 1 were considerably higher than at probe 2. For the description of the characteristic features of the curves, the induced currents at both probes were again simulated. A best fit was obtained by a three particle model with $N=3$ (Fig. 3, right curves) assuming that the number of agglomerations, their size, and relative delay were identical at both probes. In order to fit the experimental results quantitatively, the velocities and the minimum distances were approximated from the experimental data to

$$v_{\text{probe 1}}/v_{\text{probe 2}} = 0.2 \quad \text{and} \quad h_{\text{probe 1}}/h_{\text{probe 2}} = 0.5.$$

On the basis of this simulation, the following interpretation of the experimental results appears to be reasonable: Particles in the bend of the hose exhibited an averaged velocity of 1/5 compared to particles in the straight parts. This decrease of the average velocity along the hose could be explained by impact of the friction force on the particle con-

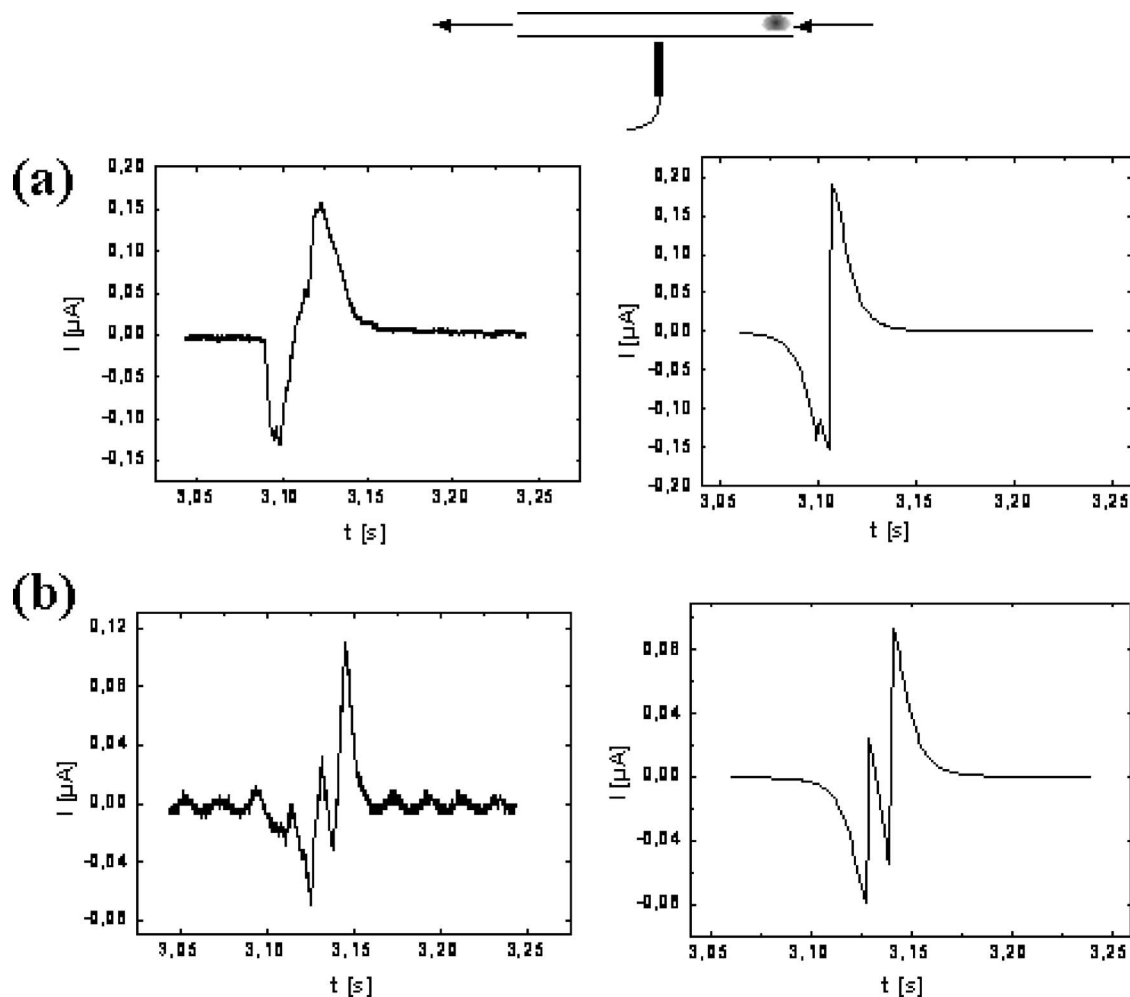


FIG. 2. Top: schematic representation of the applied experimental geometry for laser printer toner particles moving in a straight hose. Left column: experimentally determined induced currents. Right column: simulated curves assuming a two particle model ($N=2$) with $Q=\text{const}$. (a) $Q_1/Q_2=0.3$; $\Delta t=4$ ms; $h/v=5$ ms; (b) $Q_1/Q_2=0.7$; $\Delta t=6$ ms; $h/v=5$ ms.

tacting the tube surface. This smaller velocity resulted in a broadened current peak. On the other hand, the change in velocity was attributed to a higher frictional force on the walls of the tube caused by the centripetal acceleration of the particles that follow the circular path. The particles were pressed harder against the wall in the bend, so that the minimum distance h was reduced by the factor of 2. The electric field and correspondingly the induced polarization of probe 1 were increased, which led to a higher maximum of the induced current at the probe.

B. Straight collision of microparticles with a dielectric wall

The straight collision of microparticles with a dielectric wall [acrylic glass, boron silicate glass (JENAer GLAS™)] was also investigated. The setup of this experiment is shown in Fig. 4 (top scheme). Again, a typical experimentally measured curve (Fig. 4, left) and the corresponding simulated curve (Fig. 4, right) of the induced current at the probe nearby the reflection point are shown. The measured induced current was described by the proposed simulation model with $N=2$. The particles moving towards the probe were reflected into the opposite direction after the collision. The

particle velocity changed its sign after this reflection, so they passed the probe again in the opposite direction, in analogy to the velocity in the straightened hose when the particles were passing the probe. This resulted in similarly shaped current curves (compare Figs. 4 and 2). Interestingly, the reflection of particles from the wall occurred with negligible additional triboelectric charging, which was concluded from the same absolute current values of the negative and positive peak maxima.

C. Microparticles in a conical tube and in a cyclone

In the following experiments, geometries that intensified the microparticle contact with surfaces were considered, as they might be used to create strongly charged particles. Typical examples for such geometries were a conical tube and a cyclone.

The charging behavior of laser printer toner particles was investigated in a conical soda-lime glass tube. The tube was about 12 cm long with its diameter linearly decreasing from 2.5 to 0.7 mm. This conical shape of the tube continuously intensified the contact of the microparticles with the walls of the tube. The metal wire probe for current measurement was located in the middle of the tube, as similarly

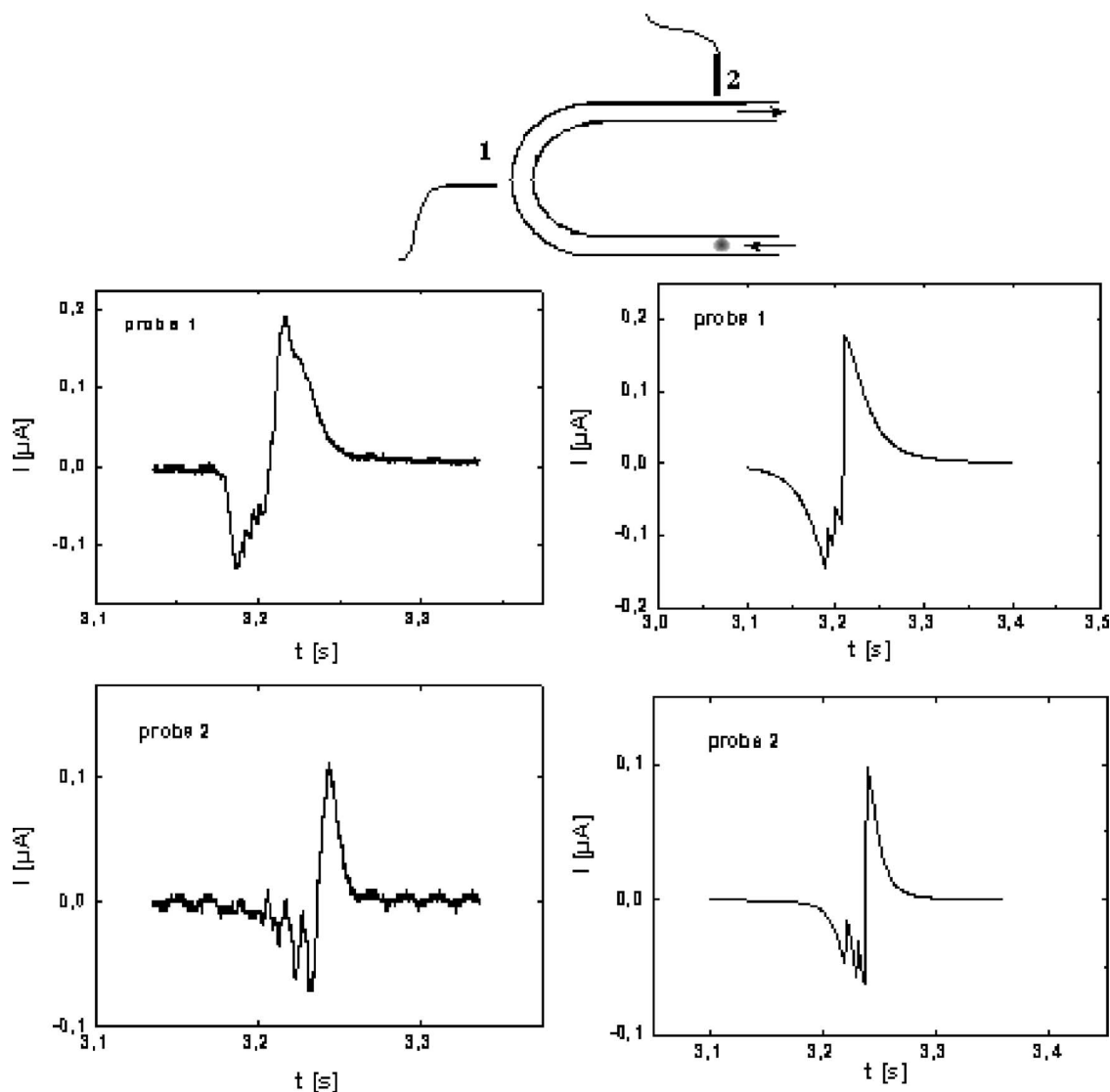


FIG. 3. Top: schematic representation of the applied experimental geometry for laser printer toner particles moving in a bent hose with two probes. The induced currents at probe 1 in the bend and at probe 2 in the straight region of the hose are shown (left column: experimental data; right column: corresponding simulations). Both model curves were simulated with $N=3$ and the same relative charges and delays of the particles. For v and h the following approximations were derived from the experimental data: $v_{\text{probe1}}/v_{\text{probe2}}=0.2$; $h_{\text{probe1}}/h_{\text{probe2}}=0.5$.

shown in Fig. 2 (top scheme). The experimentally determined and simulated induced current curves are shown in Fig. 5. The high asymmetry in the absolute current intensity of the experimental curve indicated $Q_{\text{ind}} > 0$ caused by an additional triboelectric charging of the particles during the probe passage.

This measured curve was simulated by means of Eq. (3) using $\eta=0.55$ (Fig. 5, right). The total induced current was the sum of the induced current by triboelectric charging on the surface [first summand in Eq. (3)] and the induced current of the moving particle [second summand in Eq. (3)]. It is interesting to notice that this experimentally obtained dependence cannot be described by $\eta=0$, i.e., only with the second summand of Eq. (3), although this term includes the charge dependence on the time.

Another setup for increasing triboelectric charging is sketched in Fig. 6 (top image). With an air stream, laser printer toner particles were injected edgewise into a cylinder made of acrylic glass with a diameter of 15 mm. Thus, the

particles described a helical curve in the cylinder before leaving the cylinder. The wire probe was located at the helical particle path behind the particle inlet. This geometry resulted in a small negative peak of the induced current when the particles were approaching the probe followed by considerably increased positive peaks of the departing particles (Fig. 6). As the integral of the induced current over time Q_{ind} was positive, the particles were charged negatively. The first negative peak of the curve in Fig. 6 describes the straight approach of the initially negatively charged particles to the probe through the aperture into the cylinder. The next positive peak of the curve was interpreted by the sum of the induced currents caused by further negative triboelectric charging and helical motion of the charged particles departing the wire probe. The second positive peak indicated another cycle of negatively charged particles at the exit of the cylinder with a smaller velocity of the particles resulting in peak broadening.

Simulating such microparticle movements in a cylinder,

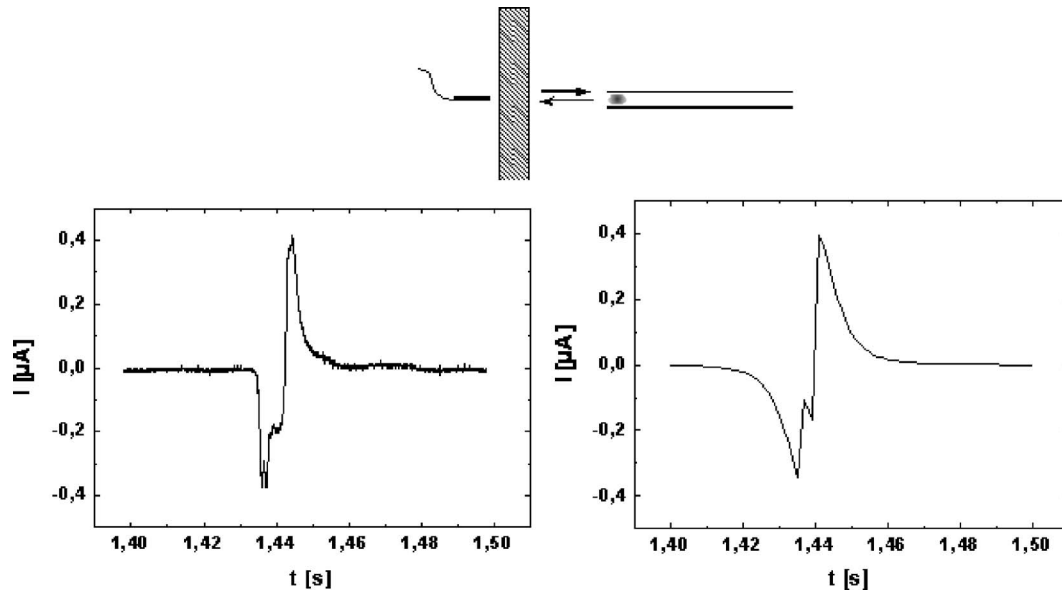


FIG. 4. Top: schematic representation of the applied experimental geometry for laser printer toner particles reflected at a dielectric wall. The experimentally measured curve of the induced current (left) and the corresponding simulation curve (right) were obtained for a collision of laser printer toner particles with an acrylic glass surface (parameters applied for the simulation: $N=2$; $Q_1/Q_2=0.5$; $\Delta t=4$ ms; $h/v=10$ ms).

it is important to consider the three dimensional geometry and orientation of the wire probe, because here the induced currents during rotation and straight motion generally depend on the three dimensional polarization of the probe.

IV. DISCUSSION

In this article a noncontact and noninvasive procedure for the analysis of electric charging conditions and motion of microparticles is presented. This method is based on the measurement of induced currents in grounded metal wire probes in combination with computer simulations. For proof of principle experiments under typical flow geometries (dielectric straight and bent hoses, conical tubes, wall collision, and a cyclone), laser printer toner particles of different colors were used. No qualitative differences were observed in the charging behavior of toner particles of different colors in all typical setups shown. The charging conditions were predominantly determined by the shape of the hose or tube and thus the resulting particle path.

For the interpretation of the data, a model for a qualitative description of the measured induced current was developed and simulated for the typical experimental conditions. In this model, the formula for the induced current was derived from the calculation of the time dependent polarization of a probe in an electric field of moving particles. Although the model assumptions of $N=2$ or $N=3$ particles appeared to be a strong simplification of the problem, the model curves well fitted the given experimental conditions and resulted in reasonable explanations of the motion and charging conditions. Thus, fitting any measurements by such computer simulation curves may be used for comparison of experimental data to appropriate calibration standards. If a more precise description by the simulated curves is required, however, the geometry and the nonhomogeneity of the electric field near to the probe must be taken into account, and accurate adjustment would be allowed by evaluating the polarization vector of the probe in the nonhomogenous electric field. The latter can be calculated with Poisson's equation. The microscopic

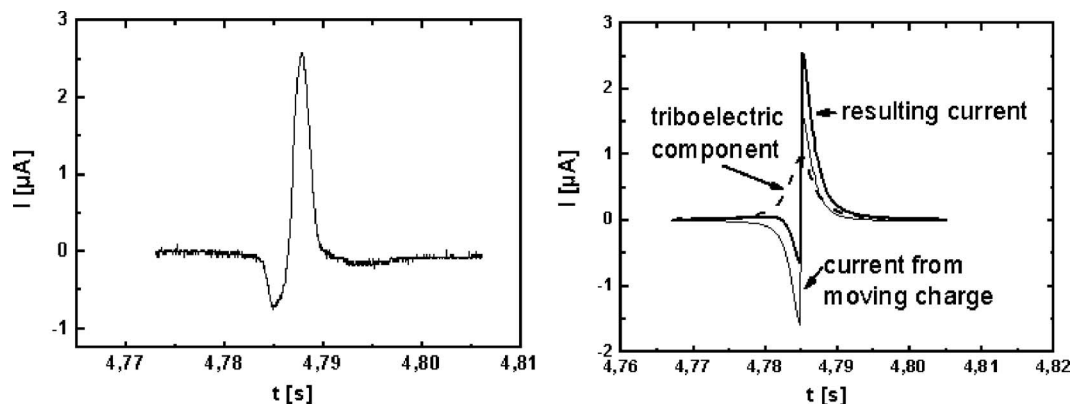


FIG. 5. The induced current at a wire probe experimentally determined during particle motion in a conical tube (left), and corresponding simulated curve (right). The simulated induced current ("resulting current") is the sum of the induced current of the moving charge (right, normal line) and the induced current resulting from triboelectric charging (right, dashed line).

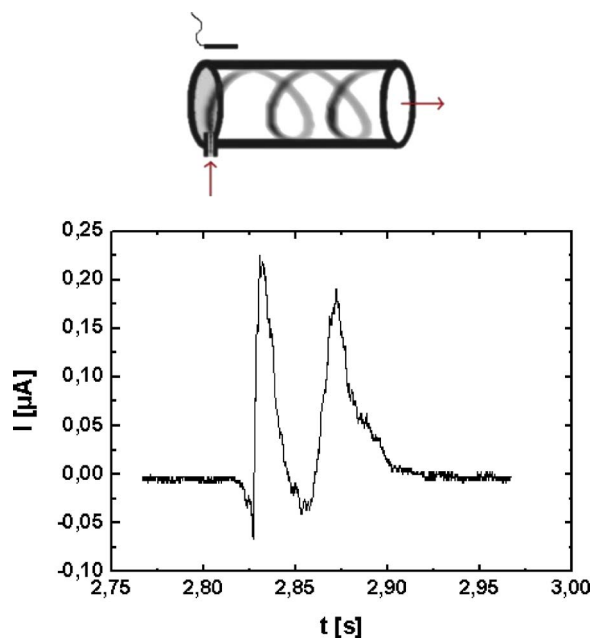


FIG. 6. Top: schematic representation of the applied experimental geometry for laser printer toner particles moving on a helical path in a cylinder. The data show the measured induced current at the probe for particle movement in an acrylic glass cyclone.

meaning of the coefficient η used in Eq. (3) might also be of further interest. While the simulation data clearly show the necessity of this coefficient, which may characterize surrounding air (gas) discharging effects usually accompanying triboelectric charging of microparticles, it also has been shown to be appropriate for correcting these effects.

Taken together, the experimental method and simulation tool proposed can be used as a reliable system for the analysis and control of triboelectric properties of different materials, including polymers or biodegradable carriers in many

experimental setups for material sciences and biomedical research. Such applications are, for instance, the production of high complexity peptide or DNA arrays that are used for screening purposes in systems biology.

ACKNOWLEDGMENT

The financial support of the German Federal Ministry for Education and Research (BMBF) is gratefully acknowledged.

- ¹G. Mainelis, K. Willeke, P. Baron, S. A. Grinshpun, and T. Reponen, *Aerosol Sci. Technol.* **36**, 479 (2002).
- ²W. W. Nazaroff and G. R. Cass, *Atmos. Environ., Part A* **25A**, 841 (1991).
- ³C. J. Weschler, H. C. Shields, and B. M. Shah, *J. Air Waste Manage. Assoc.* **46**, 291 (1996).
- ⁴Y. J. Suh and S. S. Kim, *J. Aerosol Sci.* **27**, 61 (1996).
- ⁵A. Desai, S.-W. Lee, and Y.-C. Tai, *Sens. Actuators, A* **73**, 37 (1999).
- ⁶H. O. Jacobs and G. M. Whitesides, *Science* **291**, 1763 (2001).
- ⁷S. Jilek, M. Ulrich, H. P. Merkle, and E. Walter, *Pharm. Res.* **21**, 1240 (2004).
- ⁸*Aerosol Science*, edited by C. N. Davis (Academic, New York, 1966).
- ⁹E. Nemeth, dissertation, Technischen Universität Bergakademie, Freiberg, 2003.
- ¹⁰J. Lowell and A. R. Akande, *J. Phys. D* **21**, 125 (1988).
- ¹¹D. K. Davies, *IAS Annual Meeting, 1980* (IEEE, New York, 1980), Vol. II, p. 1038.
- ¹²E. M. Charlson, E. J. Charlson, S. Burkett, and H. K. Yasuda, *IEEE Trans. Electr. Insul.* **27**, 1144 (1992).
- ¹³L.-H. Lee, *J. Electrostat.* **32**, 1 (1994).
- ¹⁴P. H. W. Vercoulen, J. C. M. Marijnissen, and B. Scarlett, *J. Aerosol Sci.* **26**, 797 (1995).
- ¹⁵J. B. Gajewski and A. Szaynok, *J. Electrostat.* **10**, 229 (1981).
- ¹⁶Y. Yan, *Meas. Sci. Technol.* **7**, 1687 (1996).
- ¹⁷H. Masuda, T. Komatsu, N. Mitsui, and K. Iinoya, *J. Electrostat.* **2**, 341 (1977).
- ¹⁸S. N. Murnane, R. N. Barnes, S. R. Woodhead, and J. E. Amadi-Echendu, *IEEE Trans. Instrum. Meas.* **45**, 488 (1996).
- ¹⁹J. B. Gajewski, *J. Electrostat.* **15**, 81 (1984).
- ²⁰S. R. Woodhead and D. I. Armour-Chelu, *J. Electrostat.* **58**, 171 (2003).
- ²¹D. I. Armour-Chelu and S. R. Woodhead, *J. Electrostat.* **56**, 87 (2002).
- ²²<http://www.oki-osd.de>